**Supporting Information.**

Table S1. Sequence of oligonucleotides used to construct 2 nt-gapped templates.

| Oligonucleotide | 5'-3' Sequence |
|---|---|
| 66-mer | AATTCGAGCTCGCCCCGGGATCCGGCTGGGCCCCCCCCAGAAGGCA GCACAAGGGGAGGAAAAGTC |
| 86-mer | CCTTGTGCTCGCCTACGGCCATACCACCCTGAAAGTGCCCGATATC GTCTGATCTCGGAAGCCAAGCAGGGTCGGGCCTGGTTAGT |
| 71-mer | AATTCGAGCTCGCCCCGGGATCCGGCTGGGCCCCCCCCAGAAGGCA GCACAAGGGGAGGAAAAGTCAGCCT |
| 81-mer | TGCTCGCCTACGGCCATACCACCCTGAAAGTGCCCGATATCGTCTG ATCTCGGAAGCCAAGCAGGGTCGGGCCTGGTTAGT |
| 63-mer | CCTTGTGCTCGCCTACGGCCATACCACCCTGAAAGTGCCCGATATC GTCTGATCTCGGAAGCC |
| 21-mer | GCAGGGTCGGGCCTGGTTAGT |
| 58-mer | CCTTGTGCTCGCCTACGGCCATACCACCCTGAAAGTGCCCGATATC GTCTGATCTCGG |
| 26-mer | GCCAAGCAGGGTCGGGCCTGGTTAGT |
| 154 bp Bottom Strand (3'-5') | TTAAGCTCGAGCGGGGCCCTAGGCCGACCCGGGGGGGGTCTTCCGT CGTGTTCCCCTCCTTTTCAGTCGGAACACGAGCGGATGCCGGTATG GTGGGACTTTCACGGGCTATAGCAGACTAGAGCCTTCGGTTCGTCC CAGCCCGGACCAATCA |

We determined the extent of acetylation of Pol β by employing [$^{14}$C-acetyl] Coenzyme A, running p300 acetylation reaction on SDS-PAGE and doing autoradiography of dried gels. We found that while the total amount of Pol β was unchanged, the level of acetylation peaked at a ratio of 1:1:10 Pol β:p300:AcCoA (Fig. S1). This was the exact ratio used in the acetylation reactions as described by Hasan et al. as producing >95% acetylation.

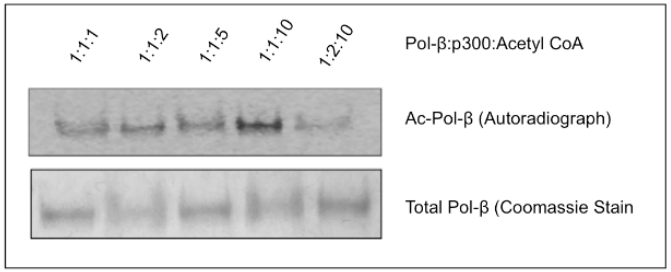


**Figure S1. Acetylation of Pol β *in vitro* using the catalytic acetyltransferase domain of p300.** Pol β was acetylated as described in the materials and methods according to a published protocol (Hasan et al., 2002). We tested different ratios of pol β:p300:acetyl CoA for optimum acetylation and found that, as previously reported (Hasan et al, 2002), pol β was maximally acetylated at ratios of 1:1:10. Interestingly, a 1:2 ratio of pol β:p300 resulted in decreased acetylation of the polymerase, presumably because of p300 quenching acetyl CoA from the reaction by autoacetylating itself (Lane 5). The lower panel shows the Coomassie stain of the separated proteins as a loading control for the acetylated protein. The same gel was subsequently exposed to a phosphor screen for 1 week, and the acetylation status of pol β was analyzed (upper panel).

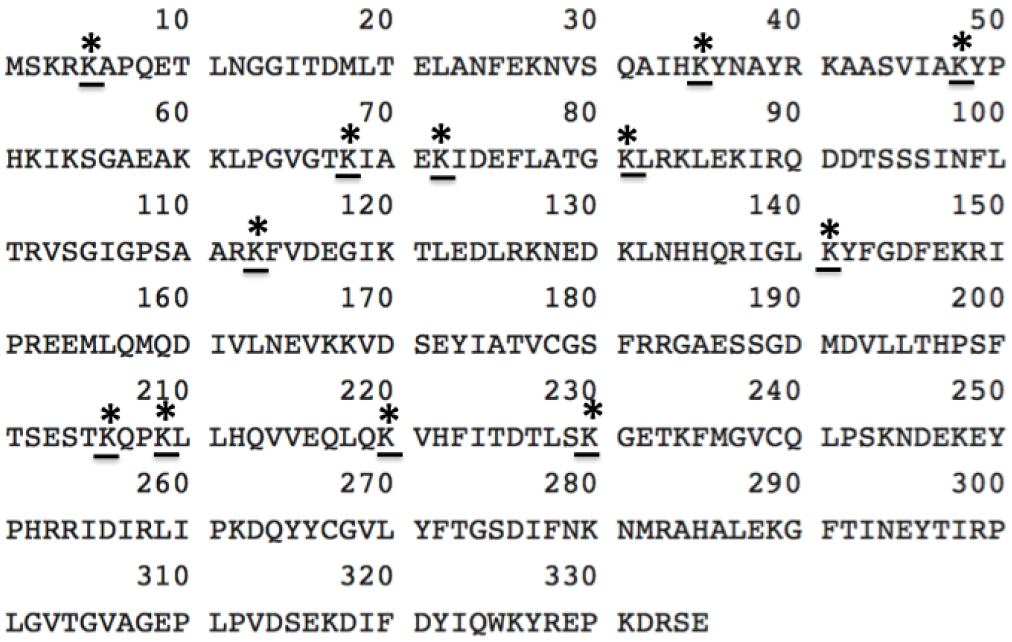


**Figure S2: Amino acid sequence of Pol β.** Sites of acetylation identified by MS are indicated by asterisks and an underline**.** All sites are lysines (K).

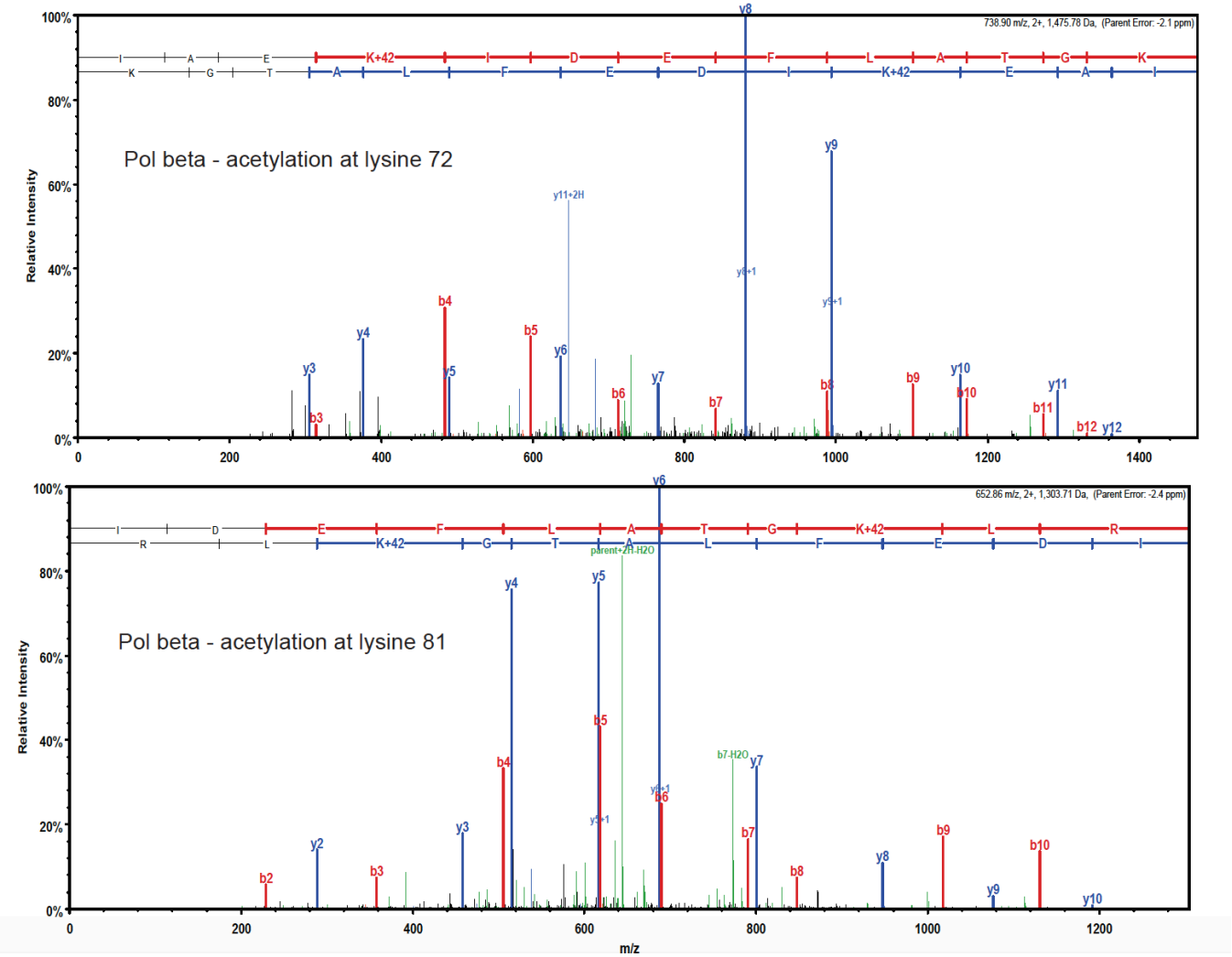


**Figure S3: Representative fragmentation spectra of acetylated lysine 72 and lysine 81 in Pol β.** The detected b- and y-fragment ion series are shown.

## Table S2: Table of Acetylated Peptide Residues of Pol β

| Sequence | Modifications | Observed | Actual Mass | Charge | Delta Da | Delta PPM |
|---|---|---|---|---|---|---|
| (R)kAPQETLNGGITDmLTELANFEK(N) | Acetyl (+42), Oxidation (+16) | 860.0928 | 2,577.26 | 3 | -0.007161 | -2.777 |
| (R)kAPQETLNGGITDMLTELANFEK(N) | Acetyl (+42) | 854.7609 | 2,561.26 | 3 | -0.00779 | -3.04 |
| (R)kAPQETLNGGITDmLTELANFEK(N) | Acetyl (+42), Oxidation (+16) | 860.0934 | 2,577.26 | 3 | -0.005147 | -1.996 |
| (R)kAPQETLNGGITDmLTELANFEK(N) | Acetyl (+42), Oxidation (+16) | 860.0922 | 2,577.25 | 3 | -0.008809 | -3.416 |
| (K)NVSQAIHkYNAYR(K) | Acetyl (+42) | 535.941 | 1,604.80 | 3 | -0.004546 | -2.831 |
| (K)AASVIAkYPHK(I) | Acetyl (+42) | 613.8459 | 1,225.68 | 2 | -0.004717 | -3.845 |
| (K)LPGVGTkIAEK(I) | Acetyl (+42) | 577.8411 | 1,153.67 | 2 | -0.003238 | -2.805 |
| (K)IAEkIDEFLATGK(L) | Acetyl (+42) | 738.8985 | 1,475.78 | 2 | -0.004992 | -3.38 |
| (K)IAEkIDEFLATGK(L) | Acetyl (+42) | 738.8995 | 1,475.78 | 2 | -0.003039 | -2.058 |
| (K)IAEkIDEFLATGK(L) | Acetyl (+42) | 738.898 | 1,475.78 | 2 | -0.005969 | -4.042 |
| (K)IAEkIDEFLATGK(L) | Acetyl (+42) | 738.8994 | 1,475.78 | 2 | -0.003161 | -2.141 |
| (K)IAEkIDEFLATGkLR(K) | Acetyl (+42), Acetyl (+42) | 894.4949 | 1,786.98 | 2 | -0.00801 | -4.48 |
| (K)IAEkIDEFLATGkLR(K) | Acetyl (+42), Acetyl (+42) | 894.4971 | 1,786.98 | 2 | -0.003493 | -1.954 |
| (K)IAEKIDEFLATGkLR(K) | Acetyl (+42) | 582.663 | 1,744.97 | 3 | -0.005574 | -3.193 |
| (K)IAEkIDEFLATGkLR(K) | Acetyl (+42), Acetyl (+42) | 596.6671 | 1,786.98 | 3 | -0.003873 | -2.166 |
| (K)IAEKIDEFLATGkLR(K) | Acetyl (+42) | 873.4901 | 1,744.97 | 2 | -0.006965 | -3.989 |
| (K)IAEKIDEFLATGkLR(K) | Acetyl (+42) | 873.4911 | 1,744.97 | 2 | -0.00489 | -2.8 |
| (K)IAEKIDEFLATGkLR(K) | Acetyl (+42) | 873.4907 | 1,744.97 | 2 | -0.005744 | -3.29 |
| (K)IAEkIDEFLATGkLR(K) | Acetyl (+42), Acetyl (+42) | 596.6658 | 1,786.98 | 3 | -0.007535 | -4.214 |
| (K)IAEKIDEFLATGkLR(K) | Acetyl (+42) | 582.6631 | 1,744.97 | 3 | -0.005208 | -2.983 |
| (K)IAEkIDEFLATGkLR(K) | Acetyl (+42), Acetyl (+42) | 596.6655 | 1,786.97 | 3 | -0.008634 | -4.829 |
| (K)IAEkIDEFLATGkLR(K) | Acetyl (+42), Acetyl (+42) | 596.6663 | 1,786.98 | 3 | -0.006253 | -3.497 |
| (K)IAEKIDEFLATGkLR(K) | Acetyl (+42) | 582.6632 | 1,744.97 | 3 | -0.004842 | -2.773 |
| (K)IDEFLATGkLR(K) | Acetyl (+42) | 652.8619 | 1,303.71 | 2 | -0.004634 | -3.552 |
| (K)IDEFLATGkLR(K) | Acetyl (+42) | 652.8626 | 1,303.71 | 2 | -0.00317 | -2.429 |
| (K)IDEFLATGkLR(K) | Acetyl (+42) | 652.8622 | 1,303.71 | 2 | -0.003902 | -2.991 |

| | | | | | | |
|---|---|---|---|---|---|---|
| (K)IDEFLATGkLR(K) | Acetyl (+42) | 435.5767 | 1,303.71 | 3 | -0.005594 | -4.287 |
| (R)kFVDEGIK(T) | Acetyl (+42) | 489.2669 | 976.5193 | 2 | -0.003876 | -3.965 |
| (R)kFVDEGIK(T) | Acetyl (+42) | 489.2674 | 976.5202 | 2 | -0.002899 | -2.966 |
| (R)kFVDEGIK(T) | Acetyl (+42) | 489.2666 | 976.5186 | 2 | -0.004547 | -4.652 |
| (R)IGLkYFGDFEK(R) | Acetyl (+42) | 679.8513 | 1,357.69 | 2 | -0.003953 | -2.909 |
| (K)QPkLLHQVVEQLQK(V) | Acetyl (+42) | 865.4988 | 1,728.98 | 2 | -0.005931 | -3.428 |
| (K)QPkLLHQVVEQLQK(V) | Acetyl (+42) | 577.3348 | 1,728.98 | 3 | -0.006249 | -3.612 |
| (K)LLHQVVEQLQkVHFITDTLSK(G) | Acetyl (+42) | 840.1358 | 2,517.39 | 3 | -0.01026 | -4.073 |
| (K)LLHQVVEQLQkVHFITDTLSK(G) | Acetyl (+42) | 630.3542 | 2,517.39 | 4 | -0.00795 | -3.157 |
| (K)VHFITDTLSkGETK(F) | Acetyl (+42) | 809.4261 | 1,616.84 | 2 | -0.003494 | -2.16 |
| (K)VHFITDTLSkGETK(F) | Acetyl (+42) | 539.9523 | 1,616.84 | 3 | -0.006071 | -3.753 |

We also addressed the potential for HMGB1 to induce stable structural alterations in the nucleosome using a FRET approach. A distinct possibility is that HMGB1 stabilizes a stable unwrapping of the DNA, which would be expected to occur from the edges of the nucleosome. We examined the DNA end-to-end distance in two different nucleosomes in the absence and in the presence of HMGB1 (**Fig. S4**). We generated DNA templates for the 154 bp 5S nucleosome and a 169 bp 601-based nucleosome using Cy3 and Cy5 labeled primers (see schematic, Fig. S2 A). The 5S nucleosome has the linker-core-linker structure of 0-N-7, while the 601 nucleosome has a designed structure of 11-N-11. As expected the 154 bp DNA template yielded a low FRET (measured as Ratio (A)) of 0.14, but efficiency was greatly increased upon nucleosome reconstitution, to about 0.32. Upon addition of HMGB1, covering a range of nucleosome:HMGB1 ratios, surprisingly HMGB1 did not detectably alter DNA end-to-end distance as detected by changes in the FRET efficiency for this nucleosome. We next repeated the experiment with a nucleosome containing two 11 bp linker DNAs, as a nucleosome with two linkers is expected to bind HMGB1 more stably [Stros, et al., 2010]. Again, we found similar results, suggesting that either HMGB1 protein exposes internal nucleosome sites by a mechanism other than DNA unwrapping or that unwrapping is accompanied by distortions in the DNA that lead to changes in relative end position that compensate for the unwinding. Alternatively, it is possible that HMGB1 does not stably alter nucleosome structure but induces more facile transition to an ‘open’ state upon incursion of a DNA binding factor.

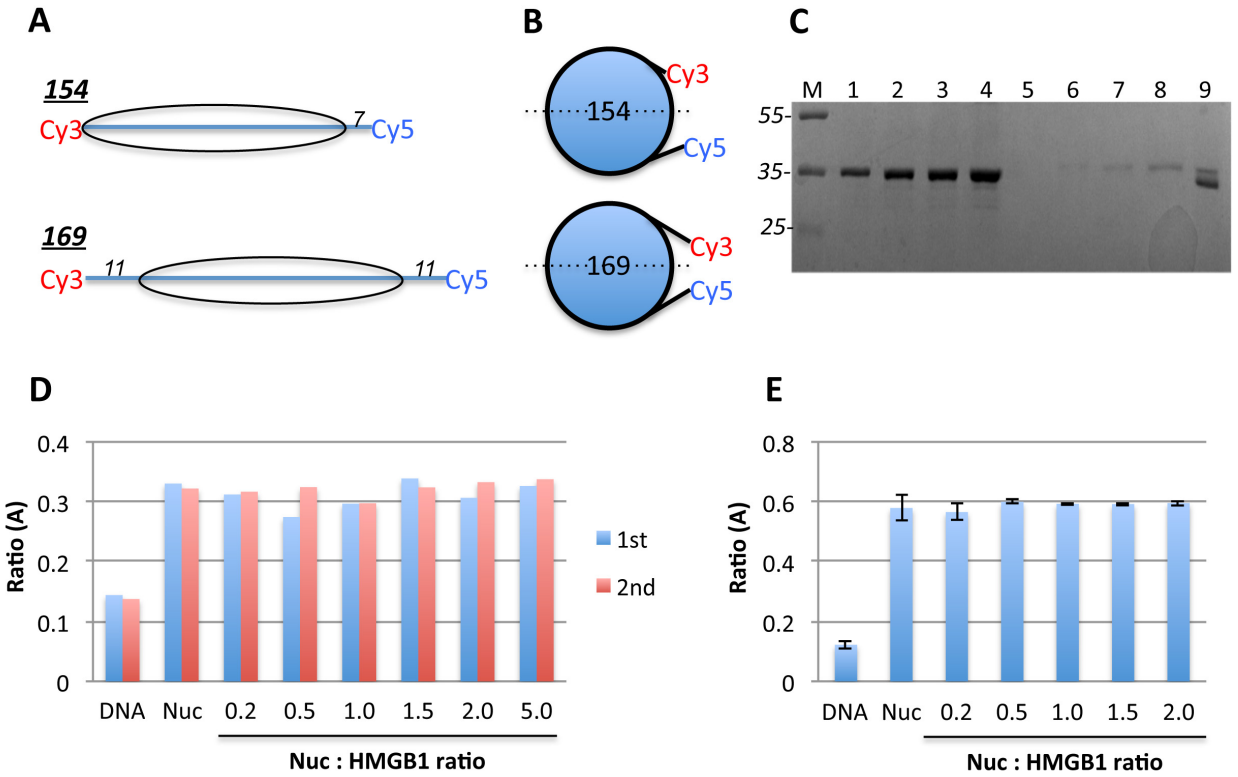


**Figure S4. Nucleosome DNA end-to-end distance does not change upon HMGB1 binding.** A. Nucleosomes were prepared using either the 154 bp 5S DNA template (see Methods) or a 169 bp 601 template labeled on each end with Cy3 or Cy5, as depicted. The former yields an asymmetric position for the nucleosome, with a single 7 bp linker, while the later yields a symmetric position with two 11 bp linker DNA segments (italic numerals). B. Expected disposition of linker DNA ends and conjugated fluorophores after nucleosome reconstitution. C. SDS-PAGE analysis of HMGB1. Lanes 1-8 contain 1.0, 1.6, 2.0, 3.0, 0.05, 0.1, 0.2, and 0.4 µg Xenopus H1.0 standard (note H1.0 is 22,500 kDa, and runs anomalously slow on SDS-PAGE). Lane 8 contains 1.2 µg HMGB1, based on densitometric comparison to the H1 standard. D and E HMGB1 binding to the 154 bp (D) or 169 bp (E) nucleosome does not alter end-to-end distance as measured by FRET. Shown are Ratio(A) values obtained for DNA alone, nucleosome alone, and a range of nucleosome:HMGB1 ratios. The concentration of DNA or nucleosomes in every sample was 20 nM. N=2 (154) or 3 (169).

**Methods:**
To generate the 169 bp 601 nucleosome we performed PCR using primers: (Forward) CY3- 5'-TCAATACATGCACAGGATGTATATATC-3' and (Reverse) CY5-5'-ACGCGGCCGCCC TGGAGAATCC-3'. Nucleosomes were reconstituted as described except that 10 ug of purified, fluorophore-labeled DNA fragment was used without carrier DNA. Nucleosomes were purified by sucrose gradient and concentrations determined by Nanodrop spectroscopy. Nucleosomes were incubated with HMGB1 in TE/50 mM NaCl and in Pol β binding buffer. FRET determinations were performed as described [Fang et al., 2016]

**SI References:**

Fang, H., et al., 2016. Chromatin structure-dependent changes of the H1 CTD. Nuc. Acids. Res. DOI:10.1093/nar/gkw586, epub ahead of print.

Hasan, S., et al., Acetylation regulates the DNA end-trimming activity of DNA polymerase beta. Mol Cell, 2002. 10(5): p. 1213-22.

Stros, M. (2010) HMGB proteins: interactions with DNA and chromatin, *Biochimica et biophysica acta 1799*, 101-113.